Chapter 3

Increasing the strength of machines under static, cyclic and dynamic loads

3.1. Increase of reliability and wear resistance of cylindrical blocks with surface plastic deformation

Aleksandr Dykha[1], Dmitry Marchenko[2]
[1]Khmelnitsky National University, Khmelnitsky, Ukraine
[2]Mykolaiv National Agrarian University, Mykolaiv, Ukraine
E-mail: [1]*tribosenator@gmail.com*, [2]*marchenkodd1984@gmail.com*

Abstract. The study of the efficiency of hardening the parts working in spalling conditions through reeling with rollers were performed with the help of physical simulation and showed the high effect of hardening cast steels. Electrography examination has shown that an increase in the degree of work hardening when reeling with a needle roller manifests itself in a higher dislocation density and cell size decrease in the substructure of ferrite grains. Diffusion of chemical elements in the surface layer in the process of surface deformation was studied with an analysis of the change of the surface microhardness. The process of the contact friction surface wear during reeling with consideration of slippage was investigated. It was proved that roughness of the friction surfaces affects the coefficient of friction and the rate of tribo-contact wear during reeling with slippage. A procedure for determining conditions of reeling with a wedge roller was developed. Optimal reeling conditions were found due to experiment planning using the steep convergence method. The obtained results of calculations will serve as initial data in designing working elements of the reeling devices and developing technological processes for strengthening parts. The conducted studies will find their future use in evaluation of the wear processes taking.

Keywords: contact strength, wear, surface plastic deformation, wedge roller, rope block.

1. Introduction

The problem of increasing wear resistance, contact strength and resistance to contact spalling is becoming increasingly relevant as intensity of handling equipment operation is constantly increasing. The most economical extension of the rope block service life is possible by improving properties of the surface layer. Surface properties can be controlled by changing the surface layer structure and physical and mechanical properties.

When operating equipment for general technical purposes, large-sized steel parts that perceive contact loads, such as cable blocks, tackle blocks, pulleys, etc. often fail. Significant work forces in the presence of misalignment of interconnected parts often bring about spalling and wear of the working friction surfaces, shape distortion, alteration of clearances between the parts. As a result, service life of handling equipment and machinery units in general is reduced. Application of thermal or thermochemical strengthening methods in the manufacture of large size rope blocks is limited by their dimension and weight. The most simple, available, and often solely possible, method for strengthening such blocks is surface processing by cold plastic working, namely reeling or hammering. To improve appearance and increase wear resistance of the surface layer, finishing surface plastic deformation (SPW) is applied and in order to increase fatigue strength and contact strength of parts, work hardening is used. Therefore, the study of the effect of the reeled surface layer properties on tribotechnical characteristics is an urgent scientific and technical problem.

2. Literature review and problem statement

During operation of rope blocks, rope interacts with the surface of the block groove. Because of elastic deformation and torsion of the rope under load, it slips and rotates round its axis. This brings about various types of damage: the groove wear, appearance of cracks, collar spalling, general deformations, and other flaws. A fundamental contribution to the theory, calculation, and design of a “rope block – rope” friction couple is made in [2]. The proposed theoretical

calculations in the design of the "rope block – rope" friction couple have low accuracy because of numerous simplifications and assumptions in the calculation method.

The issues of wear, study of surfaces subjected to contact loading as well as improvement of physical properties of surface layers are considered in [3-5]. These studies do not take into account the phenomenon of slippage of contact friction surfaces which in turn affects the mechanism of wear of the tribological couple.

The use of cast iron for casting the blocks increases wear resistance of the block by 10-12 % compared to the steel blocks. Worn cast-iron (SCh 15-32) rope blocks are replaced by blocks of steel (25L) [6]. However, the proposed methods of hardening and restoring rope blocks, namely, restoration of the blocks with the help of automatic surfacing, welding, electromechanical processing, electroplating, etc. are very costly and of a low material-output ratio. Therefore, it is more advisable to take measures to harden the rope blocks and increase their longevity, especially with the help of SFW.

When deciding on the expediency of hardening and restoration of parts, one should proceed from the technical feasibility of the enterprise in question. It is necessary to ensure performance of the part after its hardening and restoration for the entire inter-recouple service life of the unit encompassing this part and economic feasibility of hardening and restoration.

Solution of the tribo-contact problem for a friction couple was made on the basis of the wear model in [7]. The proposed solution is quite complex for practical implementation since it requires division of the wear area into discrete sections. It does not take into consideration technological features and the form of the contact friction couple.

Solution of an inverse wear contact problem for identifying parameters of the dependence of wear intensity on pressure and speed of sliding taking into account their distribution over the contact spot has been made in [8]. Based on the wear experiment by the "finger-disk" scheme, expressions for determining these parameters were obtained. However, assumption of stability of the wear spot accepted in the work in accordance with the test scheme does not make it possible to use the obtained solution for the test schemes with a variable contact (wear) spot.

A study of wear of a working "rope block – rope" friction couple caused by difference in diameters is presented in [9]. It was established on the basis of this study that the difference between the radii of the rope and the rope block profile leads to a change in distribution of contact pressures, and a phenomenon of axial slippage of the rope occurs which in turn leads to wear of the contact friction surfaces. However, the article does not present the dependence on quality of processing the friction surfaces of the "rope block – rope" couple.

The mechanism of wear of the "rope block – rope" friction couple and distribution of residual stresses in the substrate surface were studied in [10]. The results of this study indicate that the rate of wear of the alloyed steel depends on diameter of the rope wires. The mechanism of wear of annealed low-alloy steel is characterized by fatigue and abrasive wear but the wire demonstrates partial adhesion because of microabrasive wear when a fatigue crack appears. Distribution of the residual stress contacts does not depend on the motion speed. Therefore, there are constant values in the contact surface.

Analysis of the nature of failure of the parts that wear from the contact load of the friction surfaces showed that failure of rope blocks begins mostly in the surface layer and the resistance to this failure is determined by quality of the surface layer. Therefore, it is possible to influence quality of the surface layer by changing methods of surface treatment to provide predefined tribological characteristics to the friction surfaces.

Thus, further theoretical and experimental studies of physical and mechanical properties of the surface layer and microstructural studies of steel specimens after reeling them with rollers are needed. It is necessary to investigate diffusion of chemical elements in the surface layer during surface deformation by means of microchemical analysis and carry out tribological studies of wear of contact friction surfaces during reeling with allowance for slippage. All these measures will make it possible to create a method, a process, and a device for strengthening the rope blocks by

reeling and solve production problems during its implementation.

3. Materials and methods used in the tribological study of the effect of reeling parts on the contact strength

Electron microscopy studies were carried out using a UEMV-100K microscope on thin foils prepared from the specimens taken at various distances from the surface and then thinned to a thickness transparent for electrons.

Depth and degree of work hardening during plastic deformation of the surface layer were estimated using the regression analysis method. To this end, rupture tests were conducted on 0.2, ..., 0.4 mm thick flat specimens cut from a part at various distances from the part surface with the help of Shovenar machine with film recording of specimen deformation versus load diagrams.

The study of the degree of hardening with analysis of the change of microhardness and diffusion of chemical elements in the surface layer in the process of SFW was carried out as follows.

Microhardness after reeling the specimens in various conditions was determined using the PMT-3 microhardness meter. Determination of microstructure was carried out with the help of the KMT-1 device. Investigation of chemical distribution of strengthening elements by means of microchemical analysis was carried out on a raster electron microscope with the Superprobe-733 micro-X-ray micro-chemical analyzer from Jeol Company (Japan).

The study of pressure on the surface of plastic contact of the roller with the part during work hardening was carried out on 6.4 mm thick models prepared of an optically sensitive material ED6-M with the PPU-4 polarization installation (Russia).

The TRB-S-DE tribometer (Switzerland) was used in the study of wear of the contact friction surfaces during reeling taking into consideration slippage to determine tribotechnical characteristics of the “disk-sphere” friction couple and the MI wear machine was used for modeling slippage with its upper shaft rotatable to ensure transverse slip. The VLR-200 (Russia) laboratory scale was used to measure weight loss in specimens.

Experimental studies of the technological process of hardening the rope block surface by reeling were carried out on a universal 1K65 screw-cutting machine. The technological process was recorded on Panasonic SDR-S26 video camera with a subsequent frame-by-frame examination. Force on the roller varied within ±5 % since the friction force of the rolling bearings was not more than 0.008. This provided a uniform deformation of the surface layer in the rope block groove.

The degree of work hardening was measured and determined after reeling with the help of TIME Hardness Tester TH130 (India) universal integral dynamic hardness meter.

Roughness of the rope block working surface before reeling was measured using reference roughness comparison specimens OSh (GOST 9378-93 made in accordance with requirements of GOST 2789-73). After reeling, roughness was measured with the help of replicas prepared from self-curing Protacril-M plastic using the profilographer-profilometer of A1 type (GOST 19299-73 and GOST 19300-73), model 252 manufactured by Caliber Enterprise (Russia).

The reeled rope blocks were tested for spalling with ropes in production conditions on KRUPP ship reloaders (Germany) with a hoisting capacity of 40 tons, MGZ OJSC, and KS-3575 autocranes with a hoisting capacity of 10 tons, Mykolayivbudmekhanizatsiya JSC (Ukraine).

4. Results of tribological tests and process parameters of reeling steel parts with rollers

Vickers hardness under force of 0.10 kN and mechanical characteristics σ_B, $\sigma_{0,2}$ and δ were determined on specimens taken from a shaft made of 40 grade steel and reeled under a reeling force of 50.0 kN (Fig. 1).

Statistical estimation of accuracy in determining the depth of work hardening was made proceeding from the changes in hardness HV10 and the yield strength of the work hardened metal

layer. A hypothesis of normality of distribution of measurements of initial hardness and yield strength was verified by the Kolmogorov criterion. After that, the results of hardness tests were statistically analyzed by the small specimen technique.

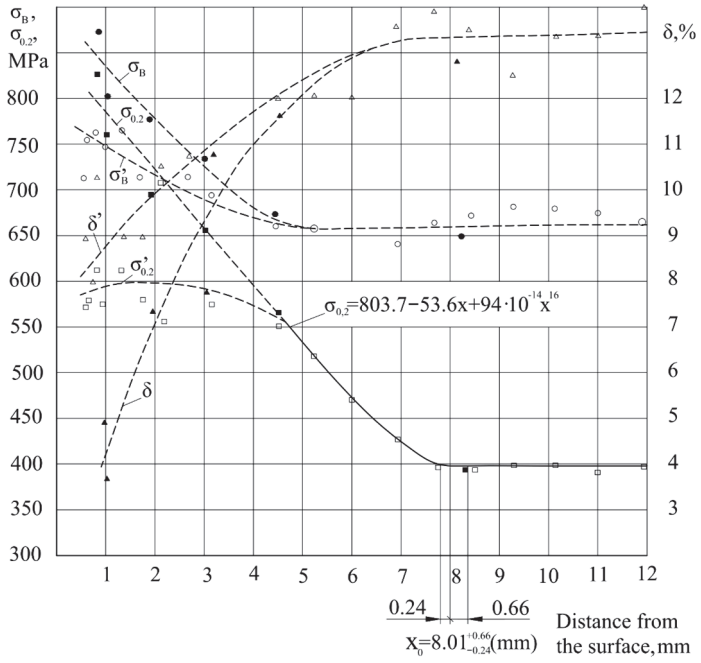

Fig. 1. Mechanical properties of the surface layer of the shafts reeled with toroidal rollers with diameter $D_p = 105$ mm, profile radius $r_p = 10$ mm: σ_B, $\sigma_{0,2}$ and δ are properties in a circular direction; σ_B, $\sigma_{0,2}$, δ are properties in the axial direction

Nonlinear regression analysis was used to determine the depth of work hardening (estimated by the start of change in mechanical properties HV10 and $\sigma_{0,2}$ of the deformed layer) and estimate accuracy of determining the depth of work hardening.

To describe the regression lines, the functions were taken [1]:

$$y = a_1 + b_1 x + b_2 x^m, \quad (1)$$

$$y = a_1 + b_1 x + b_2 \lg x, \quad (2)$$

where y is hardness or yield strength; x is the distance of the measuring point from the reeled surface.

Statistical processing of the results obtained in determining the coefficients a_1, b_1, b_2 in the regression equations was performed according to the least squares method. Dispersion coefficients, work hardening depth and its confidence intervals and the standard deviation were estimated as well.

In the process of the regression analysis, the values of coefficients of the regression Eqs. (1), (2) and the abscissa of the extremum point were initially calculated taking into account the values of mechanical properties which differed significantly from the initial ones. After the points of measuring initial mechanical properties were shifted in the direction of the x-axis, up to coincidence of their abscissas with the abscissa of the extremum point of the regression line, solution was performed again, but with taking into consideration measurements of the initial mechanical properties altered in this way.

The solution was repeated until the difference between abscissas of the points of extremum of

two last regression lines did not exceed a specified number equal to 0.01 mm. Calculations were carried out on a PC. Coefficient m of the parabolic regression line acquired values from 2 to 25.

The line having smallest residual dispersion S2 was selected from various regression lines. The best regression line has appeared to be a parabolic dependence. For all tested specimens, the hypothesis of equality of mean values of work hardening depth determined by the results of measuring hardness and yield strength checked by the Student's criterion was not confirmed.

The study results have shown that yield strength of the work hardened layer increased to a greater extent than hardness (100-130 % versus 20-60 %). Due to this, the boundary of the work hardened layer was more clearly defined by the change in the yield strength. Use of cylindrical needle rollers of a small diameter leads to a sharp increase in the deformation ratio in a thin surface layer which was indicated by grain elongation in the direction of reeling seen in the optical microphotographs.

Accuracy of determining boundary of the work hardened layer by regression analysis according to the results of measurement of yield strength is twice as high in comparison with those obtained in Vickers hardness tests. The 95 % confidence intervals for the work hardening depth calculated from the results of measurement of yield strength make up 11-36 % of the work hardening depth and 32-75 % for the hardness tests. The depth of work hardening which is determined by variations in the yield strength was 25-50 % more than the depth determined by Vickers hardness tests. This difference increases with a decrease in the degree of work hardening. The depth of work hardening determined according to the values of yield strength for circular and close to them imprints ($b/a \leq 2$) corresponded to that calculated by Heifets method even with a rather small reduced curvature of the contact between the roller and the part ($k = 0.0835$ mm^{-1}). It has been established that the yield strength was a more sensitive mechanical characteristic for determining the depth of plastic deformation than hardness. The depth of penetration of compressive stresses was close to the depth of work hardening determined by the yield strength.

Influence of conditions of reeling with rollers on the change of microstructure of the worked metal was studied in reeling with cylindrical and toroidal rollers of small diameter. Microstructure of the specimens prior to surface work hardening consists of pearlite grains surrounded by hypo-eutectoid ferrite (Fig. 2(a)). After reeling, changes in the microstructure observed on optical-digital microphotographs could only be found in the surface layers of the shaft reeled with a roller (Fig. 2(b)). The changes were seen as a considerable elongation of both ferrite and perlite grains in a circular direction of reeling. It was established that at the distance from the surface (16.42 mm), the ferrite plates of perlite din not contain dislocations. In some locations, there were isolated dislocations in the ferrite-cementite interface. Ferrite grains in the specimens were constrained by flat straight boundaries. Inside the grains, there was a three-dimensional net of low density dislocations.

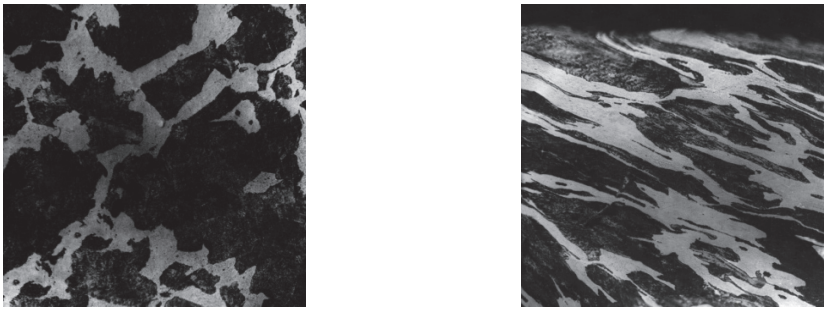

a) b)

Fig. 2. Microstructure of specimens of the surface layer of normalized 40 grade steel: a) before reeling, b) after reeling (×300)

As the electron-diffraction examination has shown, strengthening of the surface layers during

reeling shafts with a roller was mainly due to emergence of dislocation cells in the structure of the excessive ferrite grains. Higher degree of work hardening when reeling with a needle roller manifested itself by a higher density of dislocations and a reduced size of cells in the substructure of ferrite grains and a thicker grid of dislocations in the ferrite plates of perlite. In some locations, bend and fracture of cementite plates was observed which indicated the limit degree of plastic deformation of the surface layer. This was confirmed by the beginning of peeling of the surface reeled with a five-millimeter roller.

Distribution of microhardness H_μ in the depth of three specimens is shown in Fig. 3.

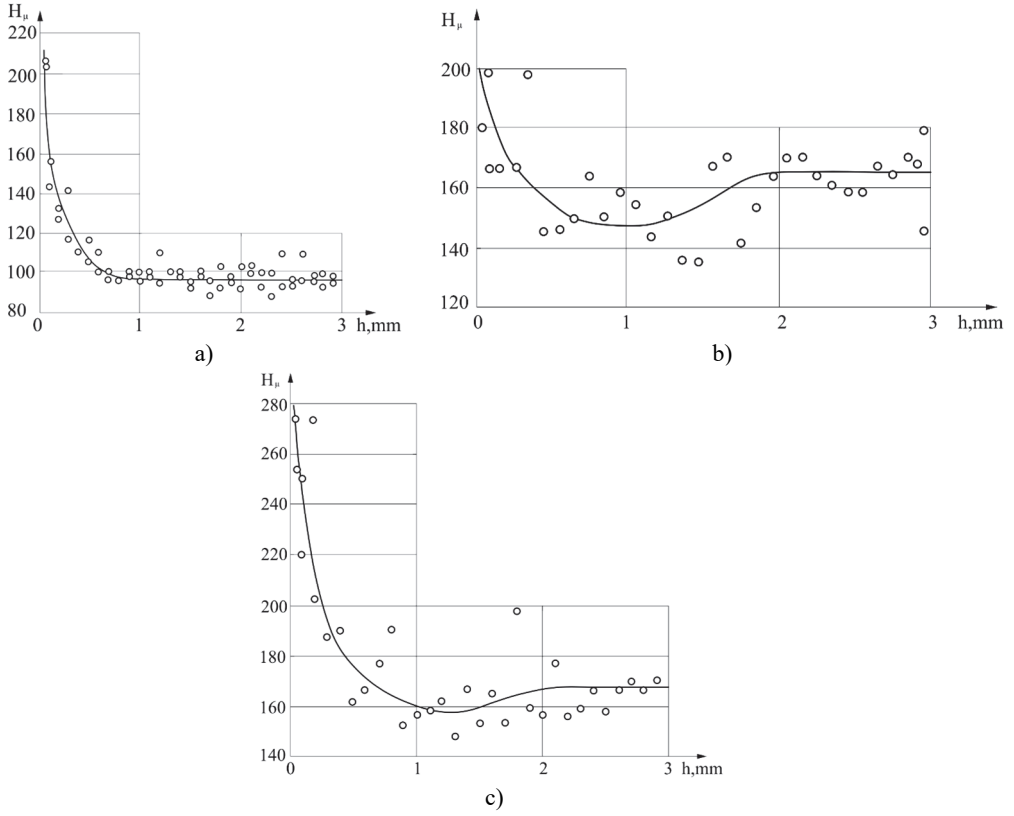

Fig. 3. Distribution of microhardness in the depth of the hardened layer: a) Armco iron, $r_p = 2.5$ mm, $P = 1.5$ kN, b) 45 grade steel, $r_p = 5$ mm, $P = 5$ kN, c) 40X grade steel, $r_p = 2.5$ mm, $P = 5.5$ kN

In the graphs of Fig. 3(b), (c) for the specimens of 45 grade and 40X grade steel, a decrease in microhardness $H_{\mu(t.z.)}$ in the transition zone between the hardened layer and the initial metal with microhardness $H_{\mu(i.)}$ was found. The average values of $H_{\mu(t.z.)}$ and $H_{\mu(i.)}$ of normally distributed values were compared with the help of t, the Student criterion.

For this purpose, the reduced variance was determined:

$$S^2 = \frac{(n_1 - 1)S_1^2 + (n_2 - 1)S_2^2}{n_1 + n_2 - 2}, \tag{3}$$

$$t = \frac{\overline{x_1} - \overline{x_2}}{S\sqrt{\frac{1}{n_1} + \frac{1}{n_2}}}, \tag{4}$$

where n_1, n_2 is the number of measurements of H_μ in the transition zone and in the initial metal, respectively; S_1^2, S_2^2 is dispersion of $H_{\mu(t.z.)}$ and $H_{\mu(i.)}$ values, respectively; $\overline{x_1}$, $\overline{x_2}$ is the mean value of $H_{\mu(t.z.)}$ and $H_{\mu(i.)}$, respectively.

If $|t| \geq t_\alpha, K$, then difference between mean values is significant. The value of the confidence probability was taken equal to 0.95, ($\alpha = 0{,}05$), the number of degrees of freedom was determined from the expression $K = n_1 + n_2 - 2$.

It was established that the content of C_r and C in the transition zone decreased by 20-30 % and increased to 10-15 % in the hardened layer. In reeling 40X grade steel and 45 grade steel, a significant reduction of microhardness was observed in the transition zone between the hardened layer and the initial metal. When Armco iron was reeled, such decrease was not detected (Fig. 3(a)). Based on these studies, a hypothesis of diffusion of strengthening chemical elements (Cr, C) from the intermediate layer to the part surface was advanced. The main mechanism of diffusion during SFW was the gradient of dislocation density.

The method of photoelasticity has shown that during elastoplastic deformations, stresses in the surface of contact of the roller with the part were distributed along a curve close to elliptic, the difference was not more than 7 %.

It was established that when slippage was up to 2 %, a sharp change in the coefficient of friction could be observed after which it remained practically constant due to the spread of slippage over the entire contact area: an obvious dependence of the value of the maximum friction coefficient on the state of the friction surface. For example, in the process of abrupt change of the coefficient of friction for hardened and not hardened specimens, with lubrication and without it, the zone (crosshatched area) was detected when running-in was achieved faster for the specimens reeled with rollers (Fig. 4(a)). It can be stated that the surface roughness only affects at small slips (up to 3 %) while reeling with rollers creates specified tribotechnical properties with reduced wear indicators in the surface layer.

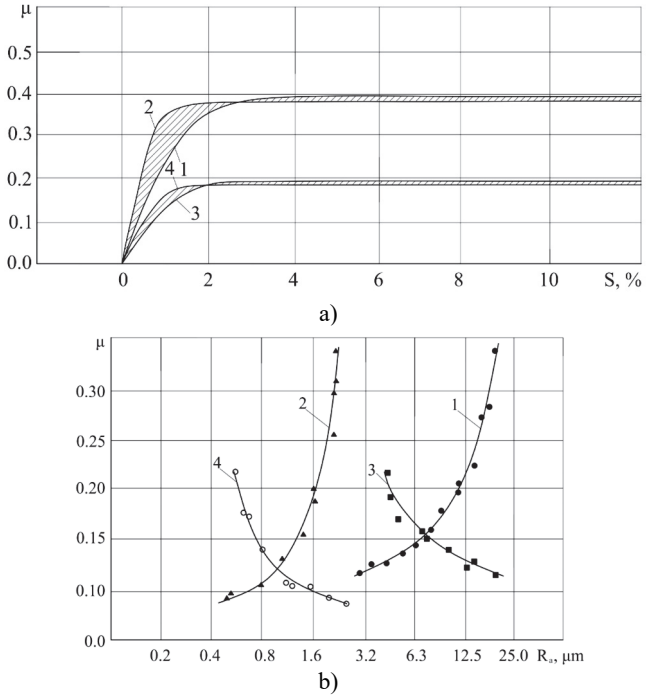

Fig. 4. a) Dependence of the coefficient of friction: on the magnitude of slip, b) on the surface roughness: non-reeled nonlubricated specimen (1); the nonlubricated specimen reeled with a roller (2); the non-reeled lubricated specimen (3); the lubricated specimen reeled with a roller (4)

Fig. 4(b) shows dependence of the coefficient of friction on the surface roughness for the specimens before reeling and after reeling with a roller and Torsiol-55 lubricant applied. It was established that with a decrease in surface roughness after reeling with rollers, lubricated specimens had a decreased coefficient of friction.

When reeling with slippage, the main mechanisms of wear were oxidizing and fatigue (spalling) wear [11, 12]. Spalling deformation increased with an increase in slippage if tangential stresses were sufficiently large.

A procedure for determining the force of reeling with a wedge roller was developed. In order to prevent excessive work hardening and peeling of the reeled metal, a limitation for the reeling force at an average angle of indentation not more than 5° was introduced. With the help of nomogram, rolling force was determined as dependent on the size of the part and the round roller and the reduced profile radius of the roller were chosen to determine the design parameters. The method of reeling steel parts [13] was developed and a theoretical analysis of geometrical parameters was made for reeling the rope blocks with a wedge roller. For this case, beating, eccentricity and diameter of the roller, its curvature, curvature of the reeled part and normal strengthening between the roller and the part in the deformation zone at all points of the profile were calculated. Calculations have shown that in order to prevent formation of waviness on the reeled surface, the profile radius r_p is made of a variable value which ensures constancy of the angle $\varphi = 5°$ of the roller indentation in all sections of the part profile.

The design of the device for reeling the rope blocks is shown in Fig. 5. It was patented, and invention patents were granted [13, 14].

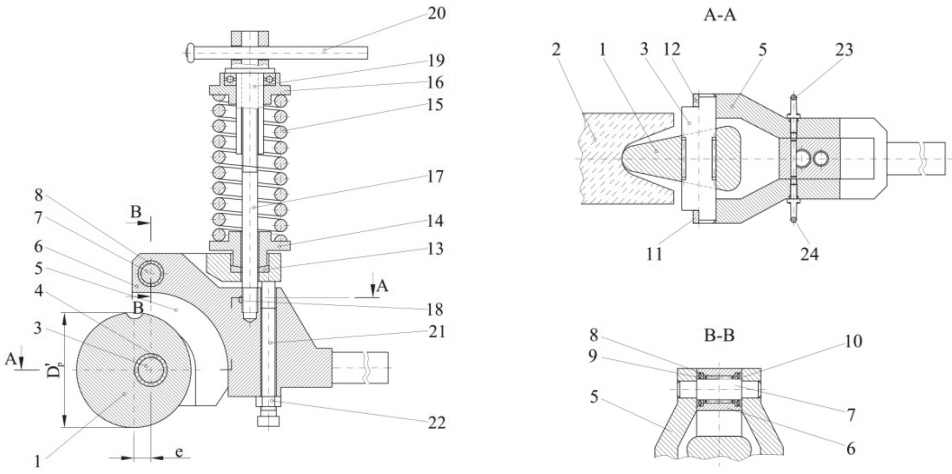

Fig. 5. The device for reeling rope blocks with a wedge roller: roller (1); reeled part (2); shaft (3, 7); bearings (4, 8, 9, 10); lever (5); bracket (6); plates (11, 12); spherical washer (13); sleeve (14); spring (15); sleeve (16); pulling rod (17); pin (18); nuts (19, 22); handle (20); screw (21); eye bolts (23, 24)

The developed device and technology of reeling [14] the rope blocks by a wedge roller provide low roughness and a high degree of surface work hardening. This effect is achieved by maintaining constant the average angle φ of the roller indentation into the surface to be worked and mounting of the roller unit on the rolling bearings. This contributes to a uniform deformation of the surface layer in absence of waviness and leads to an increase in durability of the workpiece. In the course of the experimental study, estimation of dependence of performance of the reeling process on the angle of indentation of the roller, profile radius of the roller, reeling speed and the number of revolutions of the rope block was made.

When plotting the diagram, factors were applied on the abscissa axis in an order of decreasing their rank and the sum of the ranks for the corresponding factor was applied on the ordinate axis.

With the help of the obtained diagram, an assessment of significance of the factors was made. To determine the factors that do not influence the technological process, the Student criterion (t criterion) was used. After analysis and rejection of the mentioned minor factors, a classical diagram of the ranks with a decrease in their magnitude depending on the influence of the factor on the quality of realization of the technological process was constructed. The check of significance of the expert opinions consisted in election of 10 experts, with the number of factors in the matrix being 12 and the number of degrees of freedom $f = 11$.

Analysis of expert opinions ("psychological experiment") and statistical processing have allowed us to conclude on the impact on the course and quality of implementation of the technological process. The four factors had the most affect: roller profile radius X_1, mm; speed of reeling X_2, m/min; angle of the roller indentation X_3, degrees; number of the rope block revolutions X_4, rev. The three-level, four-factor Box plan of the second order was used.

After statistical processing of the experimental data on a PC with the help of Statistica and Excel programs, mathematical models were obtained. These models were obtained for surface roughness (SR) and hardening degree (HD) which describe the technological process of reeling the rope blocks using a wedge roller device. The regression equations take the form:

$$\begin{aligned} SR = {} & 1{,}9224 - 0{,}2789 \cdot X_1 + 0{,}2520 \cdot X_2 - 0{,}5837 \cdot X_3 - 0{,}4970 \cdot X_4 \\ & -0{,}014 \cdot X_1 \cdot X_2 + 0{,}280 \cdot X_1 \cdot X_3 - 0{,}002 \cdot X_1 \cdot X_4 - 0{,}154 \cdot X_2 \cdot X_3 \\ & -0{,}522 \cdot X_2^2 + 1{,}405 \cdot X_3^2 - 1{,}280 \cdot X_4^2, \end{aligned} \quad (5)$$

$$\begin{aligned} HD = {} & 47{,}5008 - 0{,}2578 \cdot X_1 - 0{,}7167 \cdot X_2 + 0{,}135 \cdot X_3 + 0{,}1157 \cdot X_4 - 0{,}127 \cdot X_1 \cdot X_2 \\ & +0{,}236 \cdot X_1 \cdot X_3 - 0{,}535 \cdot X_1 \cdot X_4 - 0{,}124 \cdot X_2 \cdot X_3 + 0{,}115 \cdot X_2 \cdot X_4 - 1{,}062 \cdot X_3 \cdot X_4 \\ & -0{,}483 \cdot X_1^2 - 0{,}106 \cdot X_2^2 - 0{,}925 \cdot X_3^2 + 0{,}931 \cdot X_4^2. \end{aligned} \quad (6)$$

After statistical processing, analysis of the obtained regression equations was made with encoded values of factors (Table 1). Study of optimization criteria depending on the change of independent factors was carried out using the method of two-dimensional sections.

Table 1. Data of encoding the test results

Indicator	–1	0	1
X_1 – The roller profile radius, mm	10	15	20
X_2 – Speed of reeling, m/min.	20	50	80
X_3 – Angle of roller indentation, deg.	2.5	5	7.5
X_4 – Number of the rope block revolutions, rev.	100	200	300

The mathematical models were checked for the rope blocks made of steel. When analyzing the values of coefficients at factors in the regression Eq. (5), a conclusion can be drawn that the process quality is most influenced by the angle of roller indentation (X_3) and the number of revolutions of the rope block (X_4). Similarly, it can be seen from Eq. (6) that the most important are the roller profile radius (X_1) and the speed of reeling (X_2). For a more thorough study of the process, an analysis of possible combinations of pairwise combination of factors was made.

Two factors were equalized in turn to zero leaving the other two unequal to the target value. Regression equation for surface roughness and the degree of hardening at possible combinations of factors was obtained.

Equating to zero the value of the angle of roller indentation (X_3) and the number of revolutions of the rope block (X_4), regression equations were obtained in the form:

$$SR = 1{,}9224 - 0{,}2789 \cdot X_1 + 0{,}2520 \cdot X_2 - 0{,}014 \cdot X_1 \cdot X_2 - 0{,}094 \cdot X_1^2 - 0{,}522 \cdot X_2^2, \quad (7)$$

$$HD = 47{,}5008 - 0{,}2578 \cdot X_1 - 0{,}7167 \cdot X_2 - 0{,}127 \cdot X_1 \cdot X_2 - 0{,}483 \cdot X_1^2 - 0{,}106 \cdot X_2^2. \quad (8)$$

Let us take partial X_1 and X_2 derivatives and obtain a system of equations for each of the optimization criteria:

$$\begin{cases} \frac{\partial SR}{\partial X_1} = -0{,}0144 \cdot X_2 - 0{,}1886 \cdot X_1 - 0{,}2789 = 0, \\ \frac{\partial SR}{\partial X_2} = -1{,}0452 \cdot X_2 - 0{,}01440 \cdot X_1 + 0{,}25204 = 0, \end{cases} \quad (9)$$

$$\begin{cases} \frac{\partial HD}{\partial X_1} = -0{,}12771 \cdot X_2 - 0{,}96658 \cdot X_1 - 0{,}25778 = 0, \\ \frac{\partial HD}{\partial X_2} = -0{,}21326 \cdot X_2 - 0{,}12771 \cdot X_1 - 0{,}71667 = 0. \end{cases} \quad (10)$$

After solving the system of equations by each of the mathematical models, coordinates of the centers of surface response were determined for each of the optimization criteria and the value of the target function in the found YS center.

The angle of rotation of the axes in the origin of coordinates of the mathematical model was determined in a canonical form by formula:

$$\text{arctg}\, 2\alpha = \frac{B_{12}}{B_{11} - B_{22}}. \quad (11)$$

Coordinates of response of the surface centers were calculated: for the surface roughness: $X_1 = -1.49$; $X_2 = 0.26$; $\alpha = -0.96°$; $YS = 2.16$; for the degree of hardening: $X_1 = 0.19$; $X_2 = -3.47$; $\alpha = 9.36°$; $YS = 48.72$.

Coefficients of the regression equations of the characteristic equations for each of the optimization criteria were determined in a canonical form:

$$f(\lambda) = \begin{vmatrix} B_{11} - \lambda & B_{12}/2 \\ B_{21}/2 & B_{22} - \lambda \end{vmatrix} = 0, \quad (12)$$

to that end, the equations were reduced to the form:

$$\lambda^2 - I \cdot \lambda + D = 0. \quad (13)$$

Roots of this equation are the coefficients of a mathematical model in a canonical form. After the calculations, the regression equations were obtained in a canonical form:

for the surface roughness:

$$SR - 2{,}164 = -0{,}094 \cdot X_1^2 - 0{,}522 \cdot X_2^2, \quad (14)$$

For the degree of hardening:

$$HD - 48{,}7 = -0{,}096 \cdot X_1^2 - 0{,}493 \cdot X_2^2. \quad (15)$$

The results obtained by combining the X_1 and X_2 factors are shown in Fig. 6.

Consideration of the constructed diagrams makes it possible to draw a conclusion that the zone of optimal combination of factors is constrained by SR and HD curves at A, B, C, F, G points. In this case, the surface roughness will lie within 1.2 μm < SR < 1.4 μm, and the degree of hardening 44 % < HD < 45 %.

With such indicators of the optimization criteria, the value of the roller profile radius should be 16, ..., 20 mm and the speed of reeling 27, ..., 36 m min.

Consecutively changing the combination of factors, two-dimensional sections of the response surfaces were obtained for all possible combinations of factors.

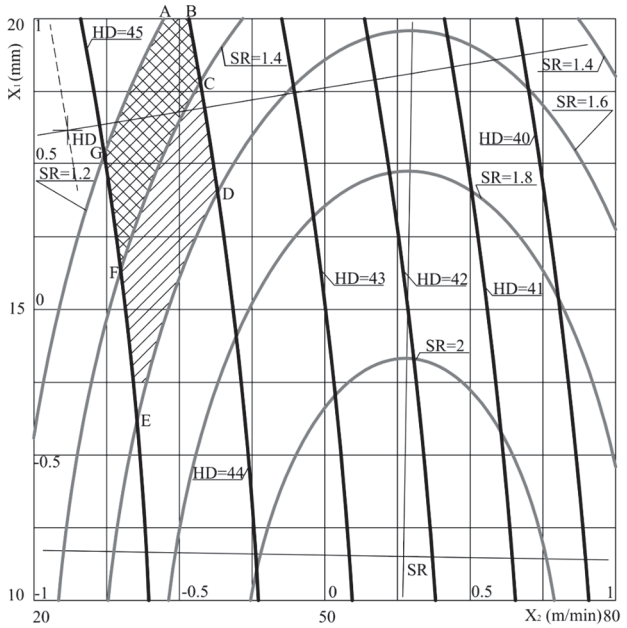

Fig. 6. Two-dimensional cross sections of the response surface after combination of the X_1 and X_2 factors at $X_3 = 0$ and $X_4 = 0$

For example, by combining the values of the angle of indentation (X_3) and the number of revolutions of the rope block (X_4) at $X_1 = 0$ (the roller profile radius) and $X_2 = 0$ (speed of reeling), the following regression equations were obtained:

$$SR = 1{,}9224 - 0{,}5837 \cdot X_3 - 0{,}4970 \cdot X_4 + 0{,}359 \cdot X_3 \cdot X_4 + 1{,}405 \cdot X_3^2 - 1{,}280 \cdot X_4^2, \quad (16)$$

$$HD = 47{,}5008 + 0{,}135 \cdot X_3 + 0{,}1157 \cdot X_4 - 1{,}062 \cdot X_3 \cdot X_4 - 0{,}925 \cdot X_3^2 + 0{,}931 \cdot X_4^2. \quad (17)$$

Solution to the system of equations has produced coordinates of the centers of the response surfaces:

– for the surface roughness: $X_3 = 0.22$; $X_4 = –0.16$; $\alpha = 3.81°$; $YS = 1.89$;

– for the degree of hardening: $X_3 = 0.08$; $X_4 = –0.01$; $\alpha = 14.8°$; $YS = 47.50$.

Fig. 7 shows results obtained for Eqs. (16) and (17) from which it is evident that the zones of the optimal combination of factors are constrained by the SR and HD curves in A, B, C and C, D, E points. In this case, surface roughness in both zones is about 1 μm, the degree of hardening is 47 % at the roll indentation angle of 4°, ..., 7° and the number of the rope block revolutions of 265, ..., 300 rev.

Significance of the obtained estimates of coefficients and the adequacy of the model was checked using the Cochran's G-criterion and the Fisher's F-criterion.

When optimizing the technological process of reeling the rope block with a wedge roller, optimum working conditions were obtained by planning the experiment. They have appeared to be the following: the roll profile radius (X_1) 15 mm, the reeling speed (X_2) 40-50 m/min, the roll indentation angle (X_3) 5 degrees, the number of the rope block revolutions (X_4) 160-180 rev. (Figs. 6, 7).

Their optimal combination forms quality of the technological process of steel part surface hardening by reeling with rollers at indicators of surface roughness (SR) of 1, ..., 1.9 μm and the hardening degree (HD) of 46.5, ..., 56 %.

Data on wear are given in Table 2.

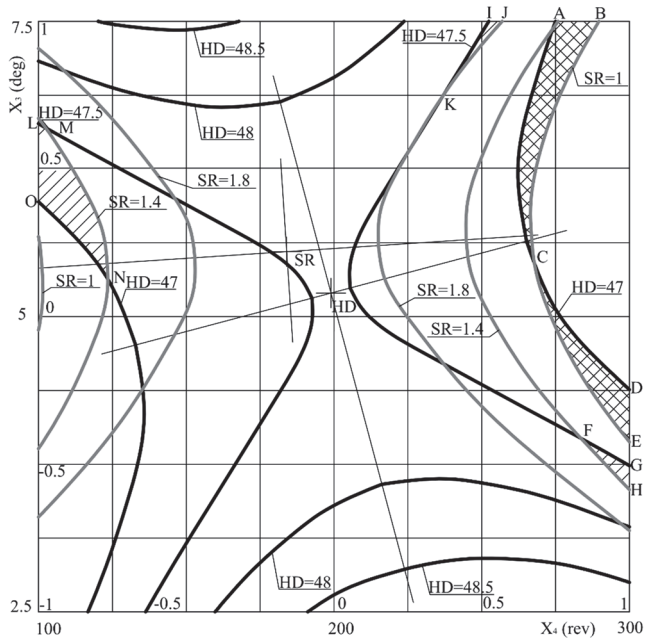

Fig. 7. Two-dimensional cross sections of the response surfaces for combining X_3 and X_4 factors at $X_1 = 0$, $X_2 = 0$

Table 2. Spalling the rope block working surface (800/120) of the KRUPP ship reloader

Wearing part	Wear, mm	Operation period, mos.	Average wear, mm/mo
Non-reeled block	4.3	4	1.0
	3.8	3	1.26
Reeled block	3.9	16	0.24
	3.2	12	0.26

It has been shown that reeling of the rope block working profile with rollers increases the contact strength and therefore imparts a 3 to 4 times higher durability. Accordingly, durability of ropes also improves as bending of the rope wires on irregularities of the worn rope block is eliminated.

The procedure of the rope block reeling to increase wear resistance and contact strength has been implemented on Krupp ship reloaders (Germany) in the cargo port of Mykolayiv Alumina Plant OJSC (Ukraine) and the auto cranes KS-3575 built by Mykolayivbudmechanizatsiya JSC (Ukraine).

5. Discussion of results of tribological studies and process conditions of reeling steel parts with rolls

Yield strength of the work hardened layer increases to a greater extent than hardness (100-130 % versus 20-60 %). Due to this, boundary of the deformed layer is more clearly found by the change of the yield strength. Use of cylindrical needle rollers of small diameter in the reeling process results in a sharp increase in the degree of deformation in a thin surface layer which is recorded on optical microphotographs as grain elongation in the direction of reeling.

Accuracy of determining boundary of the work hardened layer by the method of regression analysis using the results of measuring the yield strength is two times higher than in the case of using the results of Vickers hardness tests. The 95 % confidence intervals for the depth of work hardening with toroidal and cylindrical rollers calculated on the basis of the results of measuring

the yield strength make up 11-36 % of the depth of work hardening and the corresponding figures for hardness tests are 32-75 %.

Strengthening of the surface layers by reeling the shafts with a roller is mainly due to the emergence of dislocation cells in the structure of grains of excess ferrite. Ferrite plates of perlite show smaller deformation. Deformations of cementite plates during reeling with toroidal rollers were not detected.

An increase in the degree of work hardening by reeling with a needle roller manifests itself in a higher density of dislocations and the reduced cell size in the substructure of ferrite grains, as well as in a thicker grid of dislocations in ferrite plates of perlite. In some locations, bending and fracture of cementite plates occur indicating the extreme degree of plastic deformation of the surface layer. This is confirmed by the onset of peeling on the surface reeled with a 5 mm roller.

Diffusion of chemical elements of the surface layer in the process of surface deformation was studied. It was established that the content of Cr and C in the transition zone was 20-30 % lower and 10-15 % higher in the hardened layer. Based on these studies, a hypothesis of diffusion of strengthening chemical elements (Cr, C) from the intermediate layer to the surface of the part was put forward. The main mechanism of diffusion during SFW is the dislocation density gradient.

When reeling proceeds with slippage, the main mechanisms of wear are oxidizing and fatigue (spalling) wear. Spalling deformation increases with the growth of slippage if tangential stresses are sufficiently high.

A procedure for determining conditions of reeling the rope blocks with a wedge roller was developed. In order to prevent excessive hardening and scaling of the reeled metal, a limitation to the reeling force with an average angle of indentation not more than 5° was introduced.

The method of reeling the rope blocks and other steel parts of rotation having a complex profile was developed to improve wear resistance and contact strength [11]. Advantage of the wedge roller consists in equilibrium of the axial component of the reeling force and reeling of the working profile of the rope block is possible on horizontal and vertical lathes in a single positioning.

The device and technology of the rope block reeling with a wedge roller have been developed to provide low roughness and high degree of work hardening of the surface [12]. A set of laboratory devices was developed to determine roughness of the reeled surface by means of replicas and the degree of work hardening of the working surface. This will assist in studying physical and mechanical properties of steel parts of a complex shape working under a contact loading, including the rope blocks. This ensures obtaining of correct indicators of the technological process of work hardening using the designed device with a wedge roller.

Tribotechnical characteristics of the reeled rope blocks were defined with the help of a device with a wedge roller: the angle of indentation and the profile radius of the wedge roller, the number of revolutions of the steel rope block and speed of reeling. This has made it possible to ascertain possible limits of variation of main design and technological conditions of strengthening with the proposed device and elucidate shape of the wedge roller.

As a result of experimental study with the use of the method of steep convergence, optimal design and kinematic parameters of the reeling process were determined. Optimum working conditions were obtained by planning the experiment with optimization of the technological process of reeling the rope block with a wedge roller. They are the roller indentation angle: 5°, the roller profile radius: 15 mm, the number of the rope block revolutions: 160-180 rev., the speed of reeling: 40-50 m/min.

The optimum combination forms quality of the technological process of surface hardening of the rope blocks by reeling with rollers with the following indicators: surface roughness of 1, ..., 1.9 μm and hardening degree of 46.5, ..., 56 %.

The conducted experimental studies have proved adequacy of the results obtained in physical and mathematical modeling of the tribotechnical processes occurring during reeling the working friction surface of the rope block with a wedge roller. This allows us to recommend the developed mathematical models for their application in hardening steel parts working in conditions of wear

and action of contact forces in the mechanical engineering and other industry sectors.

It has been shown that reeling of the working profile of the rope blocks ensure a 3-4 times higher durability and contact strength and therefore service life. Accordingly, service life of ropes improves as well due to elimination of the rope wire bending over the surface irregularities of the worn rope block.

The proposed hardening technology can be used for other large-sized steel parts working in wear conditions in various industries. Tribological studies of the "rope block – rope" friction couple during reeling taking into account slippage do not provide absolute correspondence with the actual course of the wear process but is a necessary step in the development of computational engineering methods for predicting wear resistance of friction units which will facilitate development of techniques to improve their service life. Further studies in this direction should be conducted by dissemination of the proposed technology to other machinery friction units and their corresponding laboratory wear test patterns.

6. Conclusions

1. With application of the regression analysis methods, the actual accuracy of determining the depth of hardening has been estimated using the data on changes in mechanical properties of the surface layer metal. It was established that accuracy of determining the boundary of the work hardened layer according to the yield strength change is twice as high as that according to the hardness change. It was shown that the depth of work hardening which is determined according to the changes in the yield strength is 25-50 % greater than the depth determined according to the Vickers hardness change. This difference grows with the decrease in the work hardening degree.

2. Diffusion of strengthening chemical elements taking place in the surface layer during the process of surface deformation was studied. It was established that the content of Cr and C decreased by 20-30 % in the transition zone and increased to 10-15 % in the hardened layer. When reeling steel of 40X and 45 grades with rollers, a significant reduction of microhardness in the transition zone between the hardened layer and the initial metal was observed. When reeling Armco iron, this reduction cession was not detected. Based on these studies, a hypothesis of diffusion of the strengthening chemical elements C_r and C from the intermediate layer to the surface of the part due to the dislocation density gradient has been advanced.

3. A procedure for calculating the depth of work hardening for the case of reeling the part friction surface with a wedge roller was proposed and the limits of its rational application were set. An original technique of reeling steel parts was developed in order to increase their contact strength and wear resistance. This technique makes it possible to intensify the process and optimize conditions of plastic deformation, increase productivity of the reeling process, and achieve specified tribotechnical properties of the friction surfaces in large-sized steel parts.

References

[1] **Babei Y. I., Butakov B. I., Sysoev V. G.** Analysis of piezomotor driver for laser beam deflection. Journal of Vibroengineering, Vol. 11, Issue 1, 2009, p. 17-26.

[2] **Kindrachuk M. V., Kornienko A. O., Fedorchuk S. V., Tisov O. V.** Stress-deformed state of composite material loaded with friction and temperature. Problems of Tribology, Vol. 1, 2006, p. 153-157.

[3] **Aulin V., Arifa W., Lysenko S., Kuzyk A.** Improving of the wear resistance of working parts agricultural machinery by the implementation of the effect of self-sharpening. International Journal of Engineering and Technology (UAE), Vol. 5, Issue 4, 2016, p. 126-130.

[4] **Kuzmenko A. G., Dykha A. V.** Contact, Friction and Wear of Oiled Surfaces. KhNU, Khmelnitsky, 2007, p. 344.

[5] **Braude B. I., Gohberg M. M., Zvyagin I. E.** Handbook for Cranes. Mechanical Engineering. Characteristics of Materials and Loads. Basics of Calculation of Cranes, Their Drives and Metal Constructions, 1988, p. 536.

[6] **Chernets M. V.** Prediction of the life of a sliding bearing based on a cumulative wear model taking into account the lobing of the shaft contour. Journal of Friction and Wear, Vol. 36, Issue 2, 2015, p. 163-169.

[7] **Soldatenkov I. A.** Evolution of contact pressure during wear of the coating in a thrust sliding bearing. Journal of Friction and Wear, Vol. 31, Issue 2, 2010, p. 102-106.

[8] **Togawa K., Arai S., Uwatoko M.** Influence of traction sheave P.C.D. difference on sheave and rope. Journal of the Proceedings of the Elevator, Escalator and Amusement Rides Conference, 2012, p. 31-34.

[9] **Ryu J. B., Chae Y. H., Kim S. S.** A fundamental study of the tribological characteristics of sheave steel against a wire rope. Journal of the Key Engineering Materials, Vol. 297-300, 2005, p. 1382-1387.

[10] **Dykha A. V., Kuzmenko A. G.** Solution to the problem of contact wear for four-ball wear-testing scheme. Journal of Friction and Wear, Vol. 36, Issue 2, 2015, p. 138-143.

[11] **Dykha A., Aulin V., Makovkin O., Posonskiy S.** Determining the characteristics of viscous friction in the sliding supports using the method of pendulum. Eastern-European Journal of Enterprise Technologies, Vol. 7, Issue 87, 2017, p. 4-10.

[12] **Butakov B. I., Shebanin V. S., Butakova G. S., Marchenko D. D.** A Method of Finishing and Strengthening the Processing of Surfaces of the Bodies of Rotation of a Complex Profile and a Device for Its Implementation. Patent No. 93252, Ukraine, Bulletin No. 13, 2010.

[13] **Butakov B. I., Shebanin V. S., Butakova G. S., Marchenko D. D.** A Device for Finishing and Strengthening the Surfaces of Bodies of Rotation of a Complex Profile. Patent No. 2493954 Russian Federation, Bulletin No. 27, 2013.

[14] **Marchenko D. D., Butakov B. I.** Promoting contact strength of steel by rolling. Journal of Friction and Wear, Vol. 34, Issue 4, 2013, p. 308-316.

Aleksandr Dykha received Doctor of Science degree in Khmelnytsky National University, Ukraine, in 2009. Graduated from the Kyiv Polytechnic Institute in 1989 with a degree in mechanical engineering. Now he works at Khmelnytsky National University, head of the department of wear and reliability. He is editor-in-chief of international scientific journal “Problems of tribology”. His current research interests include modeling of friction and wear of machines, calculation models of reliability.

Marchenko Dmitry received Ph.D. degree in Khmelnytsky National University, Ukraine, in 2014. Graduated from the Mykolaiv National Agrarian University in 2007 with a degree in mechanization of agricultural production and hydro-melioration works. Now he works at Mykolaiv National Agrarian University, department of tractors and agricultural machinery, operation and maintenance, associate professor. His current research interests include technologies of surface hardening of parts of agricultural machines

3.2. Problems of high-rate deformation of elements of modern technology under the influence of impact and impulse loads

Yurii Vorobiov[1], Nataliia Ovcharova[2]
A. Podgorny Institute for Mechanical Engineering Problems National Academy of Sciences of Ukraine, Kharkov, Ukraine
E-mail: [1]*vorobiev@ipmach.kharkov.ua*, [2]*Natka.Ovch@gmail.com*

Abstract. The high-rate elastic-plastic deformation of the elements of modern technology is considered, it is taking into account the change of the properties of materials in the process of deformation under the action of impact and impulse loads. The use of experimental studies to determine the parameters of the dynamic properties of the material is shown. On the basis of three-dimensional models and numerical methods, an analysis of the stress-strain state of protective elements for vehicles and gas turbine engines corps under impact loads was carried out. It is shown that multilayered protective elements more effectively withstand impact loads. The analysis of parameters of technological processes of connection and separation of elements due to explosion energy is carried out. Calculation-experimental methods for analysis of deformation of cylindrical elements under impact loads are considered. The results of the research are used to ensure the dynamic strength of elements of real structures.

Keywords: shock, protective elements, high-rate deformation, dynamic material properties, experiment, three-dimensional models, numerical methods, technological processes, calculation and experimental methods.

1. Introduction

Many objects of modern technology are exposed to shock and impulse loads. Therefore, protective elements play an important role for energy, transport, aerospace and military systems. Like a protective element can be used the cladding elements of vehicles, gas turbine engine corps, protective boxes, process chambers, protective elements of military facilities, personal protective equipment, etc. Under the influence of local shock loads, a three-dimensional dynamic stress-strain state arises in them. The processes of dynamic deformation proceed in the elastic-plastic stage. In this case, it is necessary to take into account the dynamic properties of the material, which depend on deformations and strain rates [1-4]. At intense impact loads, finite deformations and displacements is occurring. Therefore, the analysis of dynamic stress-strain state (SSS) is an actual and complex problem. It requires the construction of three-dimensional mathematical models that take into account all the features of the process of high-rate deformation.

Solving the problem of the protection of civil and military installations include experimental studies of dynamic material properties, numerical studies of impact loads on the critical objects of modern technology and the development of measures to reduce the danger of dynamic loads.

2. Determination of the dynamic properties of materials

Dependencies for the dynamic properties of the material are built on the basis of experimental data. Experimental studies are carried out on flat and cylindrical samples on special stands in the range of strain rates up $5 \cdot 10$ to $5 \cdot 10^3$ s^{-1} (Fig. 1). In this case, it is necessary to take into account the variability of the deformation rate and the real dynamic loads that are registered by the inertia-free sensors.

Researches in the field of high-rate deformation of structural elements are impossible without experimental data of dynamic characteristics of materials, which reflect relationships of stresses σ and strain ε, and strain rate $\dot{\varepsilon} = \frac{d\varepsilon}{dt}$: $\sigma = \sigma(\varepsilon, \dot{\varepsilon})$. Beside that complexity of processes of

high-rate deformation occurring in the elastoplastic range requires periodical experimental check of new theoretical results in this field [3, 5].

The experimental base includes several unique installations and measuring devices (Fig. 2).

a) b)

Fig. 1. Samples for testing: a) cylindrical specimens; b) a flat multilayered specimen after failure

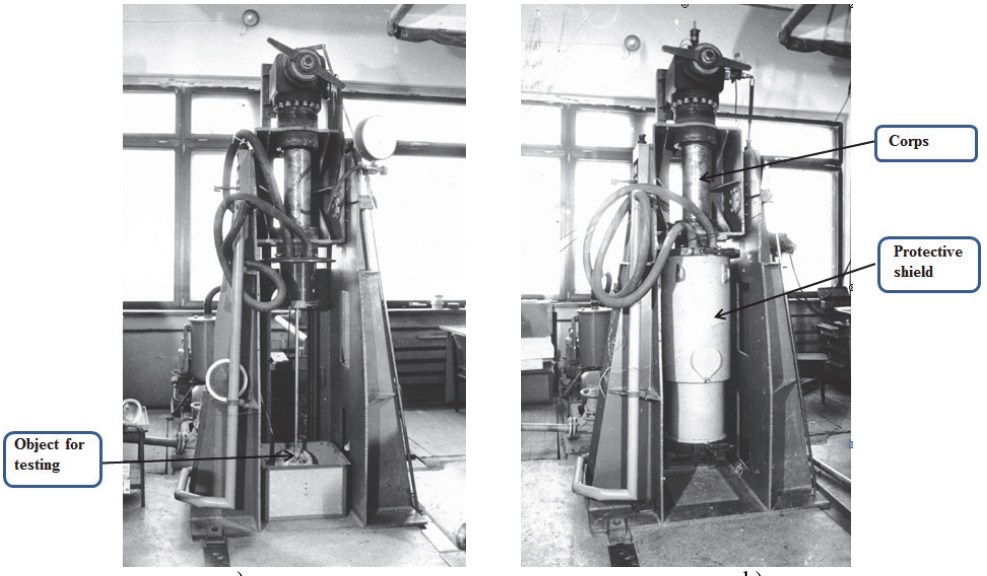

a) b)

Fig. 2. General view of the overspeed for testing samples for high-rate deformation

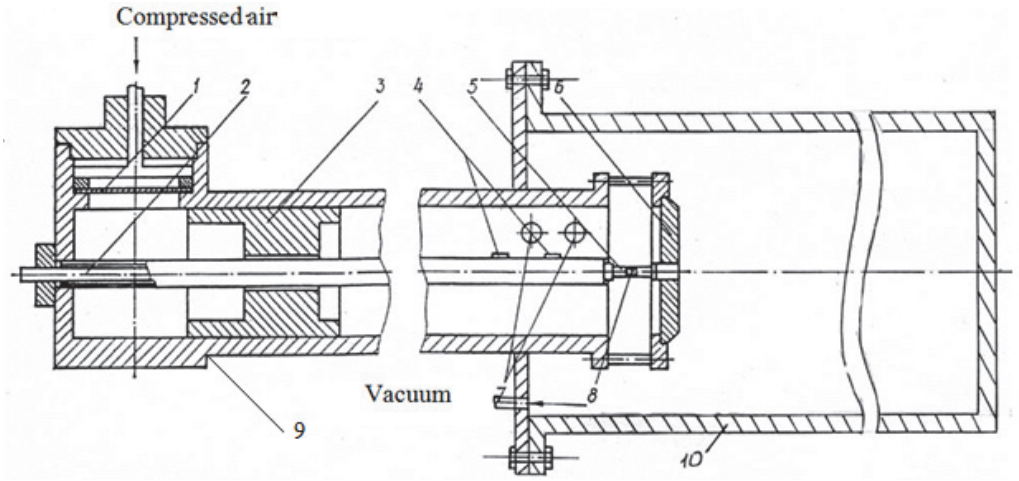

Fig. 3. Installation scheme for testing samples for high-rate deformation

Strains and strain rates are registered by small-base foil, wire or semiconductor (silicic) strain sensors. They are practically inertialess. Foil sensors operates in the rage of deformations of $\varepsilon = 0.02\text{-}0.1$ (up to 10 %) in the rage of temperatures from –200 to +500 °C. Acceleration is measured by piezoceramic sensors. Contactless vortex sensors are applied for measurement of motions. Sensors are of modulating type and operate in composition of bridges with active and reactive constituents [5].

The linear flat and cylindrical short-base specimens are tested under the conditions of high-rate uniaxial tension by the overspeed installation for determination of dynamic characteristics of material

The installation scheme is shown in Fig. 3.

Compressed air presses on the round membrane (1) with stress concentrator. The plate breaks at the predetermined pressure because of the concentrator and it provides velocities of impactor in the wide range (10-300 m/s). Under the action of compressed air hammer (3) moves in the casing (9) of 125-mm diameter till the shock on anvil (6). Specimen (5) clamped in the anvil and rod-dynamometer (2) is loaded when hammer shocks anvil. Simultaneously elastic deformations of dynamometer are registered by strain sensors (4), elastic-plastic deformations of specimen – by foil sensors (8), and hammer's speed – by pair of vortex sensors (7) and contact sensors operating from fracture. Working zone of installation is coved with protective shield (10), in which the vacuum of 10 Pa is created. Diameter of rod-dynamometer is designed of such a value that it deforms only in the elastic region and gives a force of specimen deformation $N(t)$, from which stress in specimen $\sigma(t)$ is determined. And sensor located on the specimen gives a strain of its working length $\varepsilon(t)$ [5]. Thus, relationship $\sigma = \sigma(\varepsilon, \dot{\varepsilon})$ can be plotted from the results of direct measurements without previous assumptions about the nature of specimen deformation (Fig. 4).

It is often assumed that the rate of deformation of a specimen is constant, on the basis that the kinetic energy of the impactor is an order of magnitude greater than the strain energy of the specimen. However, the process records show that this assumption is valid not at all stages of the deformation of the specimen [3, 5]. So, in Fig. 4 nonlinear sections are visible, when the sample is deformed. At hammer's speeds provided by compressed air the strain rates of $6 \cdot 10^2\text{-}6 \cdot 10^4$ s^{-1} are realized.

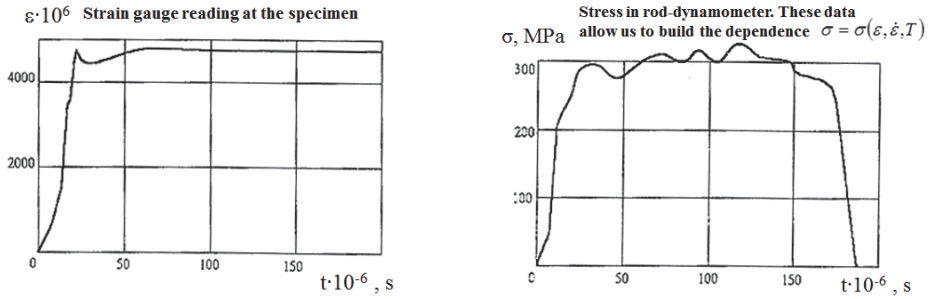

a) b)

Fig. 4. Changes of the: a) deformation of the specimen, b) stresses in the rod-dynamometer in time

To refine the dynamic characteristics of the material, the change in its cross section during deformation is takes into account (Fig. 4). Large strains (more than 10 %) when the neck is formed and the fracture of specimen are determined as the difference in the displacements of the two sections, referred to the distance between these sections $\varepsilon \approx \Delta u / \Delta x$.

Based on this measurement results, a spatial dynamic diagram is plotted in coordinates σ, ε, $\dot{\varepsilon}$. (Fig. 5).

It visually demonstrates the way of deformation of the specimen and explains the possibility of large residual deformations ε_f at a high-rate loading of the structure.

It can be seen, that the elastic limit increase with increasing deformation rate (2).

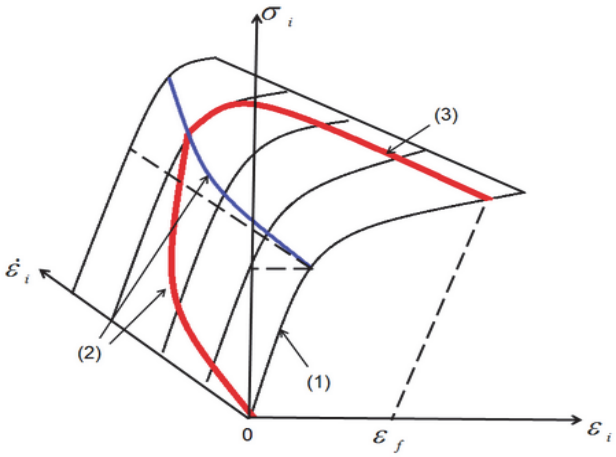

Fig. 5. The relationship between stress intensity, strain and strain rate: static deformation of the sample (1), deformation with variable speed (2), sample unloading (3),

$$(1)\ \dot{\varepsilon}_i = 0;\ (2)\ 0 \le \dot{\varepsilon}_i \le \varepsilon_s \left[1 + \left(\frac{\dot{\varepsilon}_i}{\gamma}\right)^{\frac{1}{n}}\right];\ (3)\ \Delta\varepsilon_i \le 0$$

For ease of use in the calculation of the measurement results are processed and presented in the form of a power-law dependence [5]:

$$\sigma_i = \sigma_S \left[1 + \left(\frac{\dot{\varepsilon}_i}{D}\right)^{\frac{1}{n}}\right] + \sigma_S \left\{\frac{\varepsilon_i}{\varepsilon_S}\left[1 + \left(\frac{\dot{\varepsilon}_i}{D}\right)^{\frac{1}{n}}\right]\right\}^m,$$

$$\sigma_i = \sigma_S \cdot K(\dot{\varepsilon}_i) + \sigma_S \left[\frac{\varepsilon_i}{\varepsilon_S} - K(\dot{\varepsilon}_i)\right]^m,$$

where σ_S, ε_S – static yield stresses for stresses and strains, D, n, m – parameters of high-rate material hardening.

Coefficient $K(\dot{\varepsilon}_i) = \left[1 + \left(\frac{\dot{\varepsilon}_i}{D}\right)^{\frac{1}{n}}\right]$ can be used to determine the dynamic yield stresses, strength, etc. according to their static values $\sigma_d = \sigma_S \cdot K(\dot{\varepsilon}_i)$.

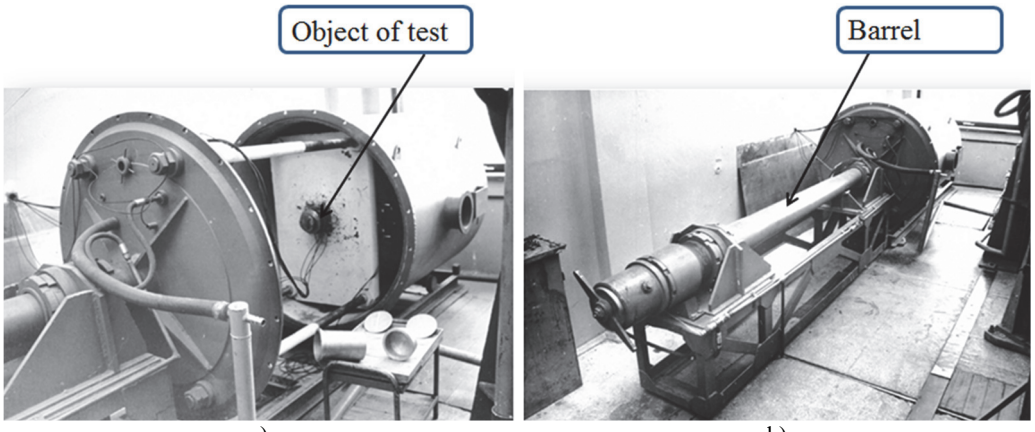

a) b)

Fig. 6. General view of overspeed installations

The installation also allows for the connection of the impactor with the deformable structure to perform a shock test, for example, shells with the ground or liquid.

For the experimental analysis of structural elements under the influence of shock loads and verification of the results of numerical analysis of the processes of high-rate deformation, a horizontal shock loading installation is used.

The general view of the overspeed installation of high-rate shock and aerodynamic loading of structural elements is shown in Fig. 6. In the shock loading mode, the impactor moves in the barrel, and in the aerodynamic loading mode, the high-rate flow of air moves in the barrel.

The diagram of the installation for aerodynamic loading is shown in Fig. 7.

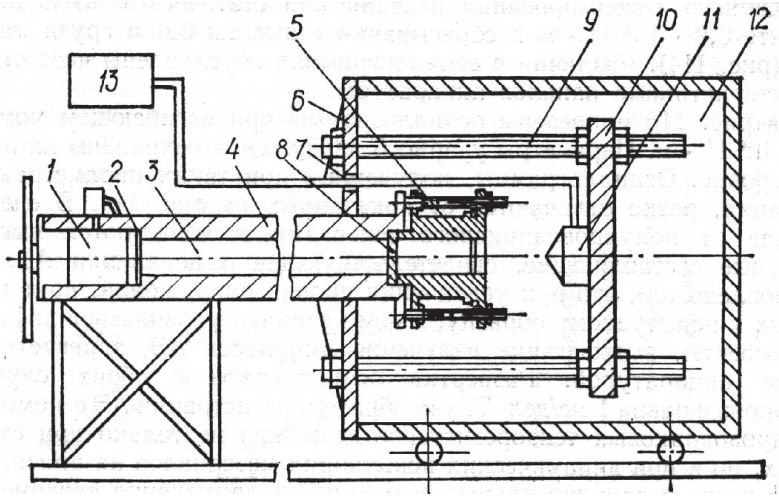

Fig. 7. Installation scheme for the aerodynamic loading regime

In the mode of shock loading the compressed air is fed into high-pressure chamber (1). At the predetermined pressure the diaphragm (2) fractures and hammer moves along the barrel of 125 mm diameter. Subject of test (11) and mounting plate (10) are located in the expansion chamber (12), connected to the barrel by flange (6). The chamber is of 1.6 m diameter and 2.2 m length with wall thickness of $\delta = 0.014$ mm allows accommodating testing subjects of sufficient dimensions. Chamber is supplied with vacuum of 10 Pa and protection of room. Compressed air provides hammer's speed up to 300 m/s [5]. The results are recorded in the measuring device (13).

In the mode aerodynamic loading the installation provides two-stage acceleration of flow by means of two diaphragms (2.8). Turbulator may be mounted on the way of aerodynamic flow.

3. Analysis of high-rate deformation of structural elements under impact.

Analytical solutions for the analysis of high-rate deformation of protective elements are achieved only in simple special cases [3, 5]. The main methods of research in this area are numerical. Ones of the most effective methods are the finite element method and the finite difference method, which take into account the specific nature of this problem. In this case, the conditions at the nodes of the finite elements and the forms functions must ensure a smooth variation of the dynamic stresses. Under the action of local loads, the zone of intense stress is very limited. Outside this zone, the stresses decrease rapidly in space and in time. Calculations in this zone can be performed with a denser grid. High-rate deformation elements of structures under the action of short-term loads of various physical nature (mechanical, impulse, shock, moving, magneto-impulse, thermal, etc.) takes place in the elastoplastic stage. It is necessary to take into account the dynamic characteristics of materials of the type $\sigma = \sigma(\varepsilon, \dot{\varepsilon}, T)$, that are obtained experimentally.

In the beginning, the behavior of elements from various materials under impact loads is studied. So, in Fig. 8 the changes of equivalent stresses in elements from various materials under the action of impactor weighing 100 g at a speed of 200 m/s are presented [6, 7].

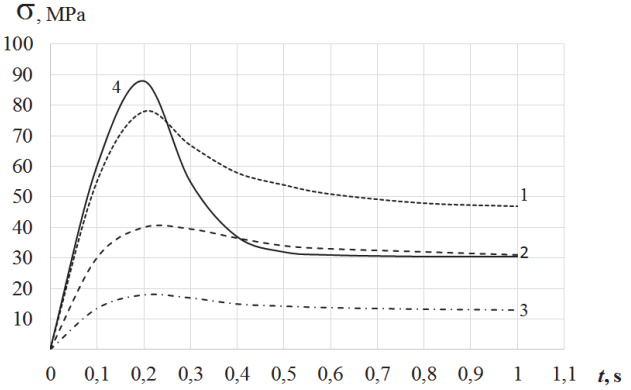

Fig. 8. Comparison of the variation of the maximum equivalent stresses for different materials: 1 – steel element; 2 – aluminum alloy, 3 – composite, 4 – titanium alloy

In the elements of steel and titanium alloy, the maximum equivalent stresses and the greatest localization of stresses are observed. The lowest stresses are observed in composite elements due to the least stiffness and large displacements.

It is allowing to select the material for protective elements or use the properties of materials of existing structures. It is shown that the elements of titanium alloys have the greatest resistance to impact loads and the growth of dynamic hardening with the impact speed, even greater than the steel samples. At the same time, the composite materials with a sufficient resistance to impact loads have the least weight.

For examples, the protective properties of vehicle lining are considered. So, for the lining of locomotives (electric locomotives), the effects of a standard impactor with weight of 100 g and with a locomotive speed of 80 km/h are considered. Also, a double impact speed, when moving oncoming trains, are interest. In Fig. 9 shows the distribution of equivalent stresses when the impactor hits an 8 mm thick fiberglass element [7].

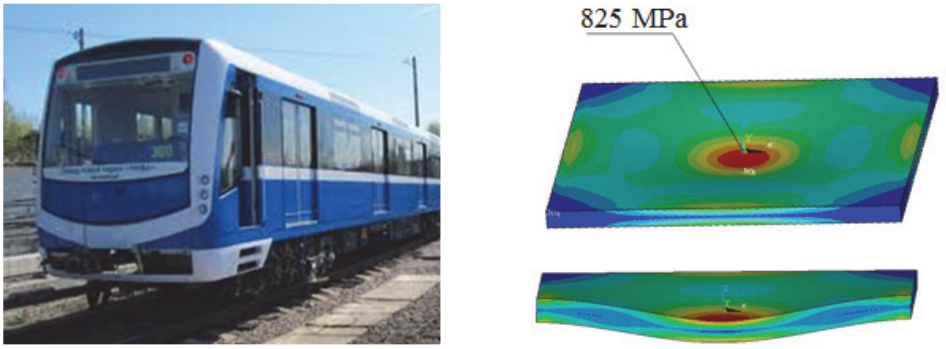

Fig. 9. The view of a locomotive and the distribution of equivalent stresses in the element of its lining under the action of impactor at a speed of 180 km/h

In this case, the largest equivalent stresses do not exceed 900 MPa, and the displacements are 1.2 mm. It can be seen that this element provides dynamic strength at speeds of up to 180 km/h.

For the facing of vehicles, the action of impactors at a speed of 60 km/h, but at different angles of encounter is considered. So, in Fig. 10 shows the displacements and stresses fields in the element of corps at an angle of 45° [7, 8].

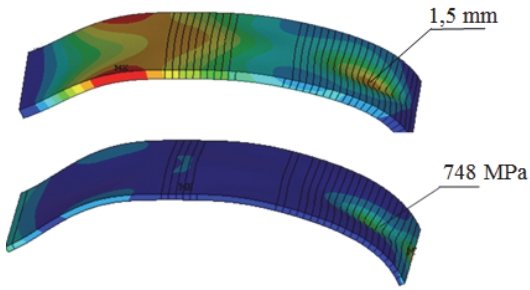

Fig. 10. Displacements and stresses in the element of the motor transport after encounter with impactor with a speed of 60 km/h at an angle of 45°

A series of similar studies show that, under impact action, the local stresses in motor vehicle corps reach significant values (up to 900 MPa) and significant deformations of the lining, but the construction retains the main operational properties at speeds of up to 60 km/h.

Of great interest is the analysis of the impact on the elements of the gas turbine engine corps of foreign objects and fragments of the compressor blades and fan blades. The effect of these impactors is interrelated. During take-off and landing of the aircraft, parts of the runway and other objects are drawn into the gas-air path of the engine, and particles of ice, moisture, sand, etc., can be drawn into when flying. These particles can cause damage of the blades. Fragments of the blades and foreign objects under the action of centrifugal forces cause impact on the engine corps. Therefore, protective elements in the form of reinforcing linings made of steel or composite materials are used in dangerous locations. Below are the results of the impact of some fragment with weight 100 g, caused by rotation of the rotor, on the protective elements of the housing. Single-layer and two-layered elements of corps are considered.

In Fig. 11 shows the distribution of equivalent stresses arising from the action of fragment of the fan blades on a protective element from composite at different times. Characteristic dimensions of the protective element: thickness 30 mm, diameter 800 mm. The rotor speed is 8500 rpm [7, 8].

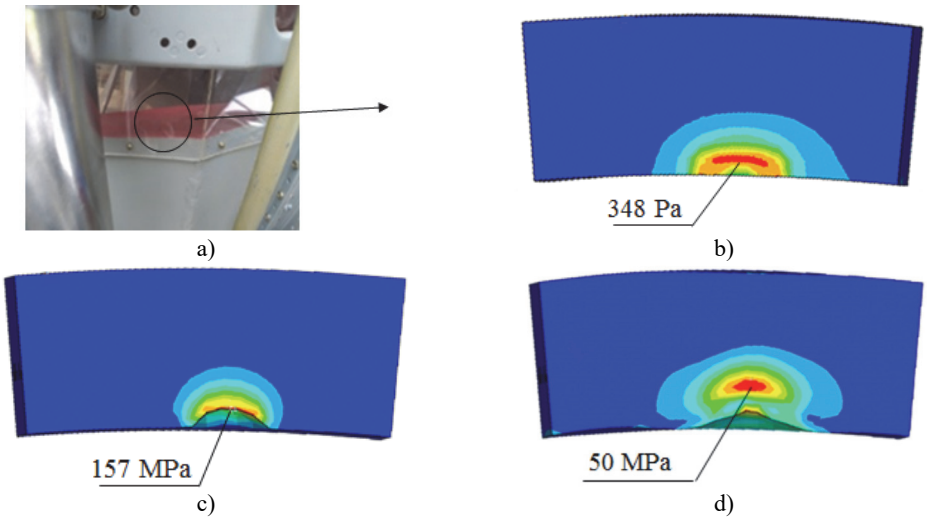

Fig. 11. Distribution of stresses in the protective element from the composite at different times at impact with a speed of 400 m/s: a) protective element from composite, b) $t = 0{,}001$ s; c) $t = 0{,}01$ s; d) $t = 0{,}1$ s

It can be seen an increase of the equivalent stresses in local zone and the formation of residual stresses and damage. The protective element does not destroy and can perform its functions even

further until repair.

At the location of the compressor blades, the elements of corps are made from steel with a thickness of 8 mm and a diameter of 415 mm. It can withstand the action of the identical impactor at a speed of 350 m/s. In this case the maximum equivalent stresses reach values of 140 MPa, and displacement of 2 mm. It is interesting, that the use of linings and double-layered protective elements significantly increases their effectiveness.

In Fig. 12 shows the distribution of equivalent stresses and displacements in a two-layer element with thicknesses of 1.4 mm and 2 mm with the same impact.

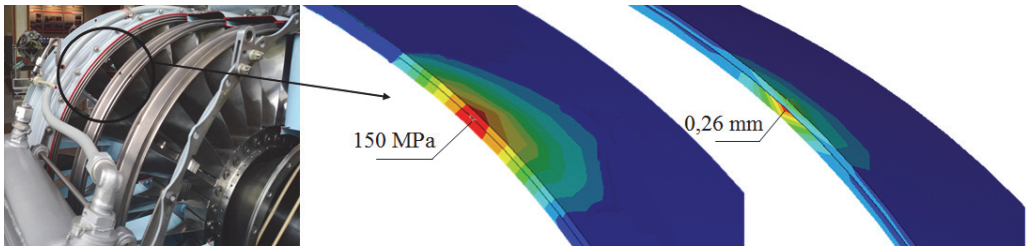

Fig. 12. Double-layered protective element and equivalent stresses and displacements in it

The maximum stresses in this case reach 150 MPa, but the total thickness of the protective element is much less than the thickness of a single-layer element [7, 8]. As the speed of the impactor increases, elastic-plastic deformations of the protective element and its damage arise (Fig. 13). For a better visualization of stresses and deformations in the element, the impactor is not shown in the figure.

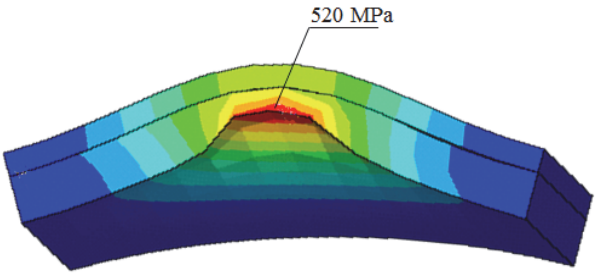

Fig. 13. Equivalent stresses in a two-layer protective element, when the impactor speed up to 1000 m/s

The presented studies show the expediency of using multilayer elements. As an example, some results of this study is given in Fig. 14. The weight of impactor is 100 g, a speed of 400 m/s; the characteristic dimensions of a three-layer target-element is 100×100 mm and the thickness of two outer layers from titanium alloy 2 mm and inner ceramic layer 3.2 mm

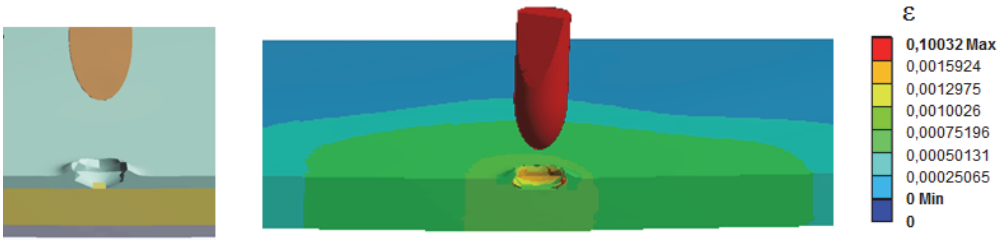

Fig. 14. Displacements and deformations in a three-layer element when the impactor speed of 400 m/s

In the top titanium layer, an area of local damage occurs, and crater formations are observed. Deformations pass into the plastic stage, and the maximum equivalent stresses reach 1330 MPa.

Local deformations in the top layer lead to the distribution of deformation in a wide region of the ceramic layer, and the stresses decrease accordingly. As a result, the impact energy is absorbed in the ceramic layer. Despite the damage of the top layer, the three-layer element retains its protective properties. A new impact occurs, as a rule, in a new location, and the element can again withstand impact. Such elements are advisable to use for light-armored vehicle and in other cases [9].

Studies have also been conducted to ensure safety during technological processes of compound and separating structural elements. For example, the processes of compounds elements by explosive energy are considered [5].

The compound of two cylindrical layers is considered. These studies should be conducted before the implementation of the relevant processes. Connections of elements occur by means of explosion welding, when the layer being thrown is connected to the target layer at a speed $3 \cdot 10^3$-$9 \cdot 10^3$ m/s due to the energy of explosive charge in sheet form, which provide a short-term (10^{-6} s) pressure $1.3 \cdot 10^{10}$ Pa. The radial displacement of the layers has the order of 10^{-4} m. The distribution of axial displacements is shown in Fig. 15.

In Fig. 16 shows the diagram of elastic-plastic deformation in the axial direction from the loading zone and the diagram of residual deformations.

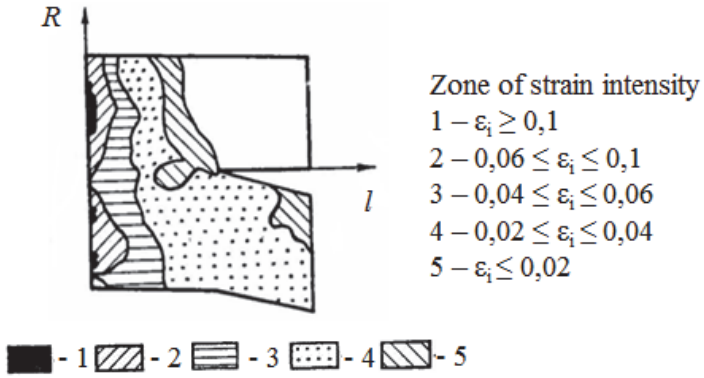

Fig. 15. The distribution of the strain intensities for the high-rate joining of two layers

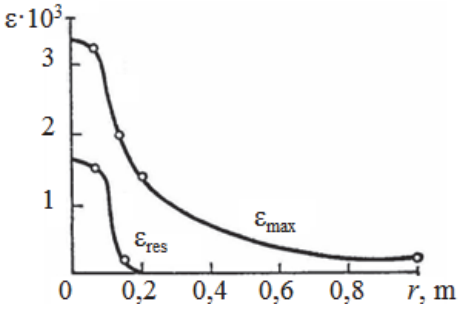

Fig. 16. The distribution of maximal (ε_{max}) and residual (ε_{res}) deformations depending on the loading zone

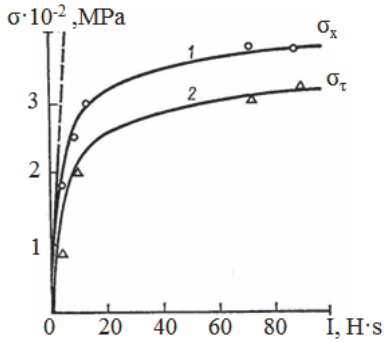

Fig. 17. Dependences of the axial (1) and circumferential (2) stresses on the loading pulse

These graphs are the boundaries in which deformations can occur during this process [5]. The process is non-linear. The dependences of the axial (1) and circumferential (2) stresses on the loading pulse I are shown in Fig. 17.

For comparison, the dotted line represents a linear relationship. The processes of explosion welding were used to combine parts of heat exchangers. A fragment of the heat exchanger at the place of compound of the tube with the elements of construction is shown in Fig. 18.

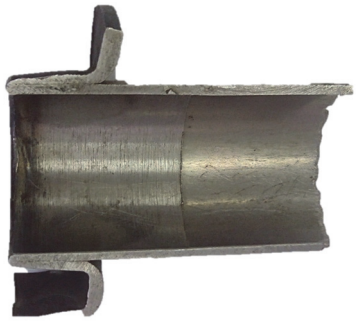

Fig. 18. A fragment of the heat exchanger at the junction of its elements by explosion welding

Also, processes of separation of elements using explosion energy are often used. In such processes, after the application of concentrators, cord explosive charges are used. In Fig. 19 shows isolines of stresses near the concentrator after 5 μs after the action of the impulse [10].

Separation processes by explosion energy were used for pulsed controlled separation of elements of space technology.

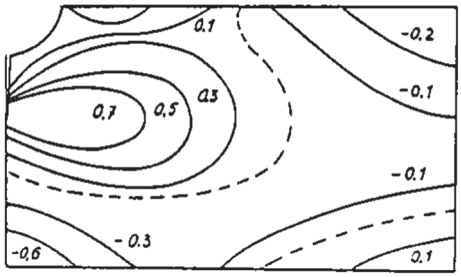

Fig. 19. The Isolines of stress (σ, GPa) near the concentrator

4. Use of the calculation-experimental method

If the properties of the materials are not sufficiently known, then the problem can be solved with the help of calculation-experimental methods. In this case, for characteristic elements, multivariate experimental studies are carried out under the actions of local loads. As a result of the processing of the experimental data, spatial dependences of the maximum values of the strain intensities on the magnitude of the impact pulse, the location of the load application, and the characteristics of the element are constructed. The methodology is based on the principles of regression analysis [11, 12]. The results of the studies are illustrated with concrete examples. As a characteristic element, cylindrical shells are chosen. Experimental studies were carried out with shells of different relative thicknesses h/R, where h – thickness, and R – shell radius. The loading was carried out with a series of loads with mass m, which were dropped on the shell from different heights, which provide different speeds of impact V, and the impulses of load mV. The deformations of the shells were measured using a system of sockets of strain sensors, which were located in the axial and circumferential directions from the loading point. Based on a series of experimental studies, a system of spatial graphs of the dependence of deformations on the parameters h/R, $I = mV$ and coordinates in the axial x and the circumferential y directions. It was assumed that the impulse load is distributed over the area of the contact region of radius c unevenly in accordance with the law:

$$P(x,y,t) = P(t)\sqrt{1-\left(\frac{x}{c}\right)^2-\left(\frac{y}{c}\right)^2}.$$

The problem of the stress-strain state is solved on the basis of Timoshenko's functional equation, the Fourier cosine-transform method with respect to the x and y coordinates, and the Laplace transform with respect to time t [11]. The structure of the solution shows that it does not have a clearly multiplicative character. Therefore, based on the processing of experimental studies, the dependence of the strain intensity $\varepsilon_i(t)$ on the parameters t, m, V, h/R, x was build. In Fig. 20 shows the spatial graphs of the dependence for $\varepsilon_i(t)$, on the surface of which lie the solution of problems for specific cases of loading.

To assess the reliability of the results, repeated experiments were carried out. Verification of the adequacy of the constructed dependence to the actual process was performed on the basis of the coefficient of multiple correlations and the Fisher test [12].

The case of impact loads on the elements of vehicles when the road milling cutters the layer of road surface is considered. When the working speed of the milling cutter is 350 rpm, the speed of the fragments is 62 m/s. Approximate weight of a typical fragment is 0.22 kg. The analysis of the deformation of gas cylinders of different sizes, which use on vehicles, under the action of shock loads was carried out (Fig. 21).

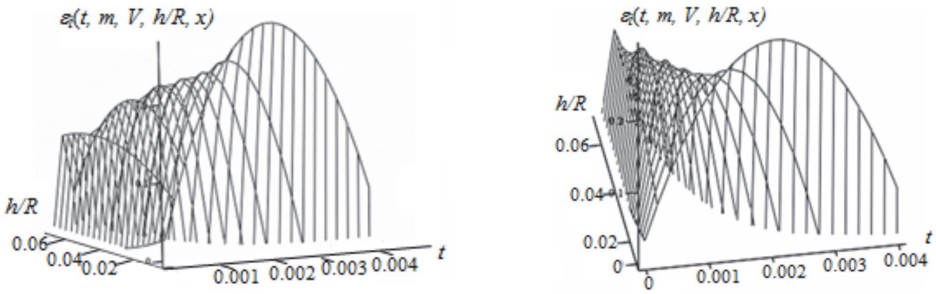

Fig. 20. Examples of surfaces on which solutions lie for different load cases

Fig. 21. General view of a road mill and vehicle with cylindrical balloon for gas

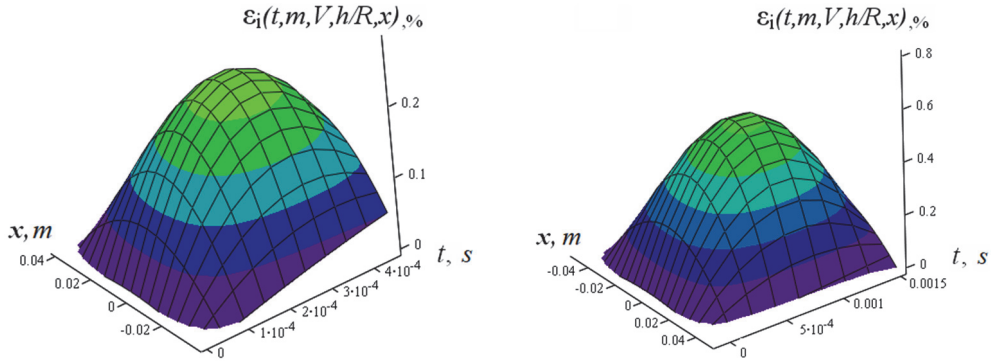

Fig. 22. Distribution of deformations around the impact zone on balloons

In Fig. 22 shows the distribution of deformations around the impact area. As an example, cylinders of different diameters and thicknesses are considered.

The maximum deformations reach 0.72 %, which is below the dynamic limit of the elasticity of the material of the cylinders. There are examples of calculations for shock loads of other cylindrical structures. Thus, by means of the calculation-experimental method, effective studies of the strength of the elements of shell structures are provided.

5. Conclusions

It is shown, that the high-rate deformation of the elements of modern structures under shock loads occurs in the elastic-plastic stage with finite displacements and changes in the properties of materials during deformation. Experiential installations for the high-rate deformation of specimens allow to determine the characteristics of the dynamic properties of materials. These characteristics are presented in the form of dependencies of stress intensities on the strain intensities and strain rates. All characteristics can change during deformation.

Investigations of the variation of equivalent stresses under shock loads in time have been carried out, which facilitates the choice of material for protective structures. The action of impact loads on protective elements is carried out using FEM based on three-dimensional models. A series of numerical studies of the dynamic stress-strain state of protective elements for vehicles and gas turbine engine corps have shown their ability to withstand shock loads in operating conditions. The advantage of multi-layered protective elements, that can withstand repeated loads, is revealed. The parameters of technological processes of compound and separation of elements with the help of explosion energy are estimated. The efficiency of the calculation-experimental method is shown, when estimating the high-rate deformation of cylindrical protective elements.

The results of the investigations make it possible to give recommendations on increasing the efficiency of protective elements of critical structures under impact and impulse loads.

References

[1] **Stepanov G. V., Babutsky A. I.** Influence of a High-Density Pulsed Electric Current on the Stress-Strain State of Metal Structural Materials. Naukova Dumka, Kiev, 2011.

[2] **Stepanov G. V., Kharchenko V. V.** Dynamic Plasticity. Mechanics of Inhomogeneous Environments. Novosibirsk, 1989, p. 285-299.

[3] **Pisarenko G. S.** Strength of Materials and Structural Elements in Extreme Conditions. Naukova Dumka, Kiev, 1980.

[4] **Meyers M. A.** Dynamics Behavior of Materials. Wiley, New York, 1994.

[5] **Vorobiov Y. S., Kolodyazhny A. V., Sevryukov V. I., Yanyutin E. G.** High-Rate Deformation of Structure Elements. Naukova Dumka, Kiev, 1989.

[6] **Vorobiov Iu. S., Kruszka L., Ovcharova N. Y.** FEM analysis of cylindrical structural elements under local shock loading. Applied Mechanics and Material, Vol. 566, 2014, p. 499-504.

[7] **Vorobiov Iu. S., Kruszka L., Ovcharova N. Y.** Sensitivity of high strain rate of structural elements in relation to dynamics properties of material. European Physical Journal Web of Conferences, Vol. 94, 2015, p. 1-3.

[8] **Vorobiov Iu. S., Kruszka L., Ovcharova N. Y.** The resistance of structural elements to impact and shock-wave load. Key Engineering Materials, Vol. 715, 2016, p. 216-221.

[9] **Vorobiov Iu. S., Ovcharova N. Y.** High-rate deformation of multilayer elements under contact impact Journal Technical Mechanics, Dnipro, Vol. 3, 2016, p. 17-24.

[10] **Vorobiov Y. S., Sevryukov V. I.** Separation of construction elements at impulse loading. Computational Plasticity, Barcelona, Spain, 1992, p. 1883-1890.

[11] **Vorobiov Y. S., Kolodyazhny A. V., Yaryzhko A. V.** High-rate elastic-plastic deformation of a cylindrical shell at a local impact. Journal Dynamics and Strength of Machines. Vol. 36, 2006, p. 40-48.

[12] **Yaryzhko A. V.** Calculation-experimental method for determine dynamics strain state of shell structures under impact load. Journal of P. Vasilenka KhNTUA. Vol. 100, 2010, p. 233-239.

Yuri Vorobiov received Dr. Sc. in dynamic and strength of machine in 1979 and Prof. in 1984 National Technical University "Kharkovskiy Polytechnic Institute", Kharkov, Ukraine. His current research interests include dynamics and strength of machines, turbomachines blading, high-rate deformation of structural elements under shocks and pulse loading taking into account elastic-plastic deformation and dynamic properties of material. He is a Secretariat member of the Ukrainian National Committee on Theoretical and Applied Mechanics; Academic of Ukraine Universities Academy; Academic of Ukraine Engineering Academy; Member of Technical Committee Rotor Dynamics of IFFToMM

Nataliia Ovcharova received Ph.D. in dynamic and strength of machine National Technical University "Kharkovskiy Polytechnic Institute", Kharkov, Ukraine in 2018. His current research interests include high-rate deformation of structural elements under shocks and pulse loading taking into account elastic-plastic deformation and dynamic properties of material. She also took part in research vibrations stress localization complex engineering constructions and turbomachines blading vibrations.